EUROPEAN ORGANIZATION FOR NUCLEAR RESEARCH

CERN-EP/89-157
December 1st, 1989

Search for the Neutral Higgs Boson from Z^0 Decay

1 December 1989

The ALEPH Collaboration

D. Decamp, B. Deschizeaux, J.-P. Lees, M.-N. Minard

Laboratoire de Physique des Particules (LAPP), IN²P³-CNRS, 74019 Annecy-le-Vieux Cedex, France

J.M. Crespo, M. Delfino, E. Fernandez[1], M. Martinez, R. Miquel, Ll.M. Mir, S. Orteu, A. Pacheco, J.A. Perlas, E. Tubau

Laboratorio de Fisica de Altas Energias, Universidad Autonoma de Barcelona, 08193 Bellaterra (Barcelona), Spain[11]

M.G. Catanesi, M. de Palma, A. Farilla, G. Iaselli, G. Maggi, A. Mastrogiacomo, S. Natali, S. Nuzzo, A. Ranieri, G. Raso, F. Romano, F. Ruggieri, G. Selvaggi, L. Silvestris, P. Tempesta, G. Zito

INFN Sezione di Bari e Dipartimento di Fisica dell' Università, 70126 Bari, Italy

Y. Chen, H. Hu, D. Huang, J. Lin, T. Ruan, T. Wang, W. Wu, Y. Xie, D. Xu, R. Xu, J. Zhang, W. Zhao

Institute of High-Energy Physics, Academia Sinica, Beijing, The People's Republic of China[12]

H. Albrecht[2], F. Bird, E. Blucher, T. Charity, H. Drevermann, Ll. Garrido, C. Grab, R. Hagelberg, S. Haywood, B. Jost, M. Kasemann, G. Kellner, J. Knobloch, A. Lacourt, I. Lehraus, T. Lohse, D. Lüke[2], A. Marchioro, P. Mato, J. May, V. Mertens, A. Minten, A. Miotto, P. Palazzi, M. Pepe-Altarelli, F. Ranjard, J. Richstein[3], A. Roth, J. Rothberg[4], H. Rotscheidt, W. von Rüden, R. St.Denis, D. Schlatter, M. Takashima, M. Talby, H. Taureg, W. Tejessy, H. Wachsmuth, S. Wheeler, W. Wiedenmann, W. Witzeling, J. Wotschack

European Laboratory for Particle Physics (CERN), 1211 Geneva 23, Switzerland

Z. Ajaltouni, M. Bardadin-Otwinowska, A. Falvard, P. Gay, P. Henrard, J. Jousset, B. Michel, J-C. Montret, D. Pallin, P. Perret, J. Prat, J. Proriol, F. Prulhière

Laboratoire de Physique Corpusculaire, Université Blaise Pascal, IN²P³-CNRS, Clermont-Ferrand, 63177 Aubière, France

H. Bertelsen, F. Hansen, J.D. Hansen, J.R. Hansen, P.H. Hansen, A. Lindahl, B. Madsen, R. Møllerud, B.S. Nilsson, G. Petersen

Niels Bohr Institute, 2100 Copenhagen, Danmark[13]

E. Simopoulou, A. Vayaki

Nuclear Research Center Demokritos (NRCD), Athens, Greece

J. Badier, D. Bernard, A. Blondel, G. Bonneaud, J. Bourotte, F. Braems, J.C. Brient, M.A. Ciocci, G. Fouque, R. Guirlet, P. Miné, A. Rougé, M. Rumpf, H. Videau, I. Videau[1], D. Zwierski

Laboratoire de Physique Nucléaire et des Hautes Energies, Ecole Polytechnique, IN²P³-CNRS, 91128 Palaiseau Cedex, France

(Submitted to Physics Letters B)

D.J. Candlin
Department of Physics, University of Edinburgh, Edinburgh EH9 3JZ, United Kingdom[14]

A. Conti, G. Parrini
Dipartimento di Fisica, Università di Firenze, INFN Sezione di Firenze, 50125 Firenze, Italy

M. Corden, C. Georgiopoulos, J.H. Goldman, M. Ikeda, J. Lannutti, D. Levinthal[19], M. Mermikides, L. Sawyer
Supercomputer Computations Research Institute and Dept. of Physics, Florida State University, Tallahassee FL 32306, USA[16,17,18]

A. Antonelli, R. Baldini, G. Bencivenni, G. Bologna[5], F. Bossi, P. Campana, G. Capon, V. Chiarella, G. De Ninno, B. D'Ettorre-Piazzoli[6], G. Felici, P. Laurelli, G. Mannocchi[6], F. Murtas, G.P. Murtas, G. Nicoletti, P. Picchi[5], P. Zografou
Laboratori Nazionali dell'INFN (LNF-INFN), 00044 Frascati, Italy

B. Altoon, O. Boyle, A.J. Flavell, A.W. Halley, I. ten Have, J.L. Hearns, I.S. Hughes, J.G. Lynch, D.J. Martin, R. O'Neill, C. Raine, J.M. Scarr, K. Smith[1], A.S. Thompson
Department of Physics and Astronomy, University of Glasgow, Glasgow G12 8QQ, United Kingdom[14]

B. Brandl, O. Braun, R. Geiges, C. Geweniger[1], P. Hanke, V. Hepp, E.E. Kluge, Y. Maumary, M. Panter, A. Putzer, B. Rensch, A. Stahl, K. Tittel, M. Wunsch
Institut für Hochenergiephysik, Universität Heidelberg, 6900 Heidelberg, Fed. Rep. of Germany[20]

A.T. Belk, R. Beuselinck, D.M. Binnie, W. Cameron[1], M. Cattaneo, P.J. Dornan, A.M. Greene, S. Dugeay, R.W. Forty, J.F. Hassard, S. Patton, J.K. Sedgbeer, G. Taylor, I.R. Tomalin, A.G. Wright
Department of Physics, Imperial College, London SW7 2BZ, United Kingdom[14]

E. Kneringer, D. Kuhn, G. Rudolph
Institut für Experimentalphysik, Universität Innsbruck, 6020 Innsbruck, Austria[22]

C.K. Bowdery[1], T.J. Brodbeck, A.J. Finch, F. Foster, G. Hughes, N.R. Keemer, M. Nuttall, B.S. Rowlingson, T. Sloan, S.W. Snow
Department of Physics, University of Lancaster, Lancaster LA1 4YB, United Kingdom[14]

T. Barczewski, L.A.T. Bauerdick, K. Kleinknecht[1], B. Renk, S. Roehn, H.-G. Sander, M. Schmelling, F. Steeg
Institut für Physik, Universität Mainz, 6500 Mainz, Fed. Rep. of Germany [20]

J-P. Albanese, J-J. Aubert, C. Benchouk, A. Bonissent, F. Etienne, R. Nacasch, P. Payre, B. Pietrzyk[1], Z. Qian
Centre de Physique des Particules, Faculté des Sciences de Luminy, IN^2P^3-CNRS, 13288 Marseille, France

W. Blum, P. Cattaneo, M. Comin, G. Cowan, B. Dehning, H. Dietl, M. Fernandez-Bosman, D. Hauff, A. Jahn, E. Lange, G. Lütjens, G. Lutz, W. Männer, H-G. Moser, Y. Pan, R. Richter, A.S. Schwarz, R. Settles, U. Stiegler, U. Stierlin, G. Stimpfl[7], J. Thomas, G. Waltermann
Max-Planck-Institut für Physik und Astrophysik, Werner-Heisenberg-Institut für Physik, 8000 München, Fed. Rep. of Germany[20]

G. de Bouard, J. Boucrot, O. Callot, X. Chen, A. Cordier, M. Davier, G. Ganis, J.-F. Grivaz, Ph. Heusse, P. Janot, V. Journé, D.W. Kim, J. Lefrançois, D. Lloyd-Owen, A.-M. Lutz, P. Marotte, J.-J. Veillet
Laboratoire de l'Accélérateur Linéaire, Université de Paris-Sud, IN^2P^3-CNRS, 91405 Orsay Cedex, France

S.R. Amendolia, G. Bagliesi, G. Batignani, L. Bosisio, U. Bottigli, C. Bradaschia, I. Ferrante, F. Fidecaro, L. Foà[1], E. Focardi, F. Forti, A. Giassi, M.A. Giorgi, F. Ligabue, A. Lusiani, E.B. Mannelli, P.S. Marrocchesi, A Messineo, F. Palla, G. Sanguinetti, S. Scapellato, J. Steinberger, R. Tenchini, G. Tonelli, G. Triggiani

Dipartimento di Fisica dell'Università, INFN Sezione di Pisa, e Scuola Normale Superiore,56010 Pisa, Italy

J.M. Carter, B.J. Green, M.G. Green, A.K. McKemey, P.V. March, T. Medcalf, M.R. Saich, J.A. Strong[1], R.M. Thomas, T. Wildish

Department of Physics, Royal Holloway & Bedford New College, University of London, Surrey TW20 OEX, United Kingdom[14]

D.R. Botterill, R.W. Clifft, T.R. Edgecock, M. Edwards, S.M. Fisher, J. Harvey, D.L. Hill, T.J. Jones, M. Morrissey, P.R. Norton, D.P. Salmon, J.C. Thompson

High-Energy Physics Division, Rutherford Appleton Laboratory, Chilton, Didcot, OXON OX11 OQX, United Kingdom[14]

B. Bloch-Devaux, P. Colas, C. Klopfenstein, E. Lançon, E. Locci, S. Loucatos, L. Mirabito, E. Monnier, P. Perez, F. Perrier, J. Rander, J.-F. Renardy, A. Roussarie, J.-P. Schuller

Département de Physique des Particules Élémentaires, CEN-Saclay, 91191 Gif-sur-Yvette Cedex, France[21]

J.G. Ashman, C.N. Booth, F. Combley, M. Dinsdale, J. Martin, D. Parker, L.F. Thompson

Department of Physics, University of Sheffield, Sheffield S3 7RH, United Kingdom[14]

S. Brandt, H. Burkhardt, C. Grupen, H. Meinhard, E. Neugebauer, U. Schäfer, H. Seywerd, K. Stupperich

Fachbereich Physik, Universität Siegen, 5900 Siegen, Fed. Rep. of Germany[20]

B. Gobbo, F. Liello, E. Milotti, F. Ragusa[8], L. Rolandi[1]

Dipartimento di Fisica, Università di Trieste e INFN Sezione di Trieste, 34127 Trieste, Italy

L. Bellantoni, J.F. Boudreau, D. Cinabro, J.S. Conway, D.F. Cowen, Z. Feng, J.L. Harton, J. Hilgart, R.C. Jared[9], R.P. Johnson, B.W. LeClaire, Y.B. Pan, T. Parker, J.R. Pater, S. Ritz[10], Y. Saadi, V. Sharma, J.A. Wear, F.V. Weber, Sau Lan Wu, S.T. Xue, G. Zobernig

Department of Physics, University of Wisconsin, Madison, WI 53706, USA [15]

[1] Now at CERN.
[2] Permanent address: DESY, Hamburg, Fed. Rep. of Germany.
[3] Now at LeCroy, Geneva.
[4] On leave of absence from University of Washington, Seattle, WA 98195.
[5] Also Istituto di Fisica Generale, Università di Torino, Torino, Italy.
[6] Also Istituto di Cosmo-Geofisica del C.N.R., Torino, Italy.
[7] Now at FSU.
[8] Now at INFN Milano.
[9] Permanent address: LBL, California, USA.
[10] Now at Columbia University, New York, USA.
[11] Supported by CAICYT, Spain.
[12] Supported by the National Science Foundation of China.
[13] Supported by the Danish Natural Science Research Council.
[14] Supported by the UK Science and Engineering Research Council.
[15] Supported by the US Department of Energy, contract DE-AC02-76ER00881.
[16] Supported by the US Department of Energy, contract DE-FG05-87ER40319.
[17] Supported by the NSF, contract PHY-8451274.
[18] Supported by the US Department of Energy, contract DE-FC0S-85ER250000.
[19] Supported by SLOAN fellowship, contract BR 2703.
[20] Supported by the Bundesministerium für Forschung und Technologie, Fed. Rep. of Germany.
[21] Supported by the Institut de Recherche Fondamentale du C.E.A..
[22] Supported by Fonds zur Förderung der wissenschaftlichen Forschung, Austria.

Search for the Neutral Higgs Boson from Z° Decay

ALEPH Collaboration

December 1, 1989

ABSTRACT

A search for the neutral Higgs boson, using the processes $Z^\circ \to H^\circ e^+e^-$, $Z^\circ \to H^\circ \mu^+\mu^-$, $Z^\circ \to H^\circ \tau^+\tau^-$, $Z^\circ \to H^\circ \nu\bar{\nu}$ and $Z^\circ \to H^\circ q\bar{q}$, is performed on data collected by the ALEPH detector corresponding to about 11,550 events of $Z^\circ \to$ hadrons. Combining all these processes, the mass range excluded is 32 MeV to 15 GeV at 95% C.L. and 40 MeV to 12 GeV at 99% C.L. The result from this experiment is unambiguous in the context of the Standard Model.

1. INTRODUCTION

The Electroweak Theory of Glashow, Weinberg and Salam [1] has been very successful, giving many theoretical predictions that have subsequently been verified experimentally. The neutral Higgs boson [2], which plays an essential role in the theory, has however not yet been seen. It is fundamentally different from all the other known particles: its observation is essential to our understanding of the "mass" problem. Experimentally, there have been many searches, for example [3], from the decays of nuclei, π, K, B, Υ etc. Some of these searches are sensitive to the assumptions used to interpret the data. So far no limits have been reported in the search for the neutral Higgs boson above 5 GeV.

In this analysis we search for the neutral Higgs boson of the Minimal Standard Model. We use the data collected during the early running of LEP, from September 19 to November 7, 1989, which correspond to 11,550 $Z^\circ \to$hadrons. These data were taken over a range of the center-of-mass energies from 88.3 GeV to 94.3 GeV, corresponding to a total integrated luminosity of 542 nb^{-1}.

The search is carried out for the process

$$Z^\circ \to H^\circ Z^*,$$

where Z^* is a virtual Z° which decays into a fermion pair. We include in the analysis all the decay modes of the Z^*. From the Standard Model, the relative branching ratios of $Z^\circ \to H^\circ e^+e^-$, $Z^\circ \to H^\circ \mu^+\mu^-$, $Z^\circ \to H^\circ \tau^+\tau^-$, $Z^\circ \to H^\circ \nu\bar{\nu}$ and $Z^\circ \to H^\circ q\bar{q}(g)$, normalized to the total rate of H° production from Z° decays, are 3.4%, 3.4%, 3.4%, 20.1% and 69.7% respectively.

In this search, we are able to cover the mass range of the Higgs boson from a few tens of MeV to about 15 GeV. For the study below the $H^\circ \to \mu^+\mu^-$ threshold, i.e. for a Higgs mass below 212 MeV where $H^\circ \to e^+e^-$ dominates, the Higgs boson is long-lived. For this mass range, we also perform a search with the identification of isolated vertices (V°).

2. THE ALEPH DETECTOR

The ALEPH detector is described in detail elsewhere [4]. The parts of the detector relevant to this analysis are the inner tracking chamber (ITC), the large time-projection chamber (TPC), the electromagnetic calorimeter (ECAL) and the hadronic calorimeter (HCAL). A 1.5 T solenoidal magnetic field is provided by the superconducting coil surrounding the TPC and ECAL. The luminosity calorimeter (LCAL) provides energy and position measurements of the showers produced by the small angle Bhabha scattering $e^+e^- \to e^+e^-$.

The readout of the apparatus is triggered independently by several separate conditions, three of which are relevant to this study. The first demands a deposition of energy in the ECAL, such that the energy in the barrel is greater than 6 GeV or the energy in either endcap is greater than 3 GeV, or 1.3 GeV each in both endcaps. The second independent trigger requires a charged track in the ITC associated in azimuth with energy deposition of more than 1.3 GeV in ECAL. A third trigger is defined by a coincidence between any of the HCAL azimuthal segments with a corresponding azimuthal segment of the ITC. A signal in an HCAL segment is registered if signals are recorded at a penetration depth of 40 cm of iron in the barrel region or 55 cm of iron in the endcap region. A signal in an ITC segment is registered by at least 5 of the 8 cylindrical wire layers recording ionization from charged particles.

3. THE DECAY OF HIGGS BOSON

To explore the Higgs mass domain accessible at LEP, a very detailed simulation of its decays is needed. In addition to the simple decays into two massive fermions $H^\circ \to f\bar{f}$, our simulation [5] includes: (i) the first order QED and QCD corrections to the channels $H^\circ \to f\bar{f}(\gamma)$ and $q\bar{q}(g)$; (ii) the decays into two gluons via a quark-loop, and into two photons via a fermion or a W-loop; (iii) a special treatment for the hadronic decays in the mass range $2m_\pi \leq m_H < \sim 2$ GeV where perturbative QCD is not reliable.

If the Higgs mass is below the muon-pair threshold, the only possible decays are those into either two photons or into an e^+e^- pair (neutrino mass is assumed to be smaller than electron mass). In the Standard Model with three generations of quarks and leptons, the branching ratio into two photons is very small (< 1%) since the W-loop almost cancels the fermion contribution [6]. Therefore, such a light Higgs decays into an e^+e^- pair and is long-lived: its lifetime varies between 0.02 and several nanoseconds and it would be detected as an electron pair with a displaced vertex. Above the muon-pair threshold, and below the pion-pair threshold, the Higgs would decay almost exclusively into two muons at the interaction point.

In the mass domain betweem $2m_\pi$ and ~ 2 GeV, the decay of a hypothetical Higgs is dominated by the two-gluon channel, but the hadronic partial width cannot be determined with perturbative diagrams. Nevertheless, it is possible to calculate the probability of $H^\circ \to \pi\pi$, $K\bar{K}$ .... by means of QCD low energy theorems with some theoretical uncertainty [7]. Moreover, the Higgs decay into two particles dominates in this mass region and, up to 1.5 - 2 GeV, one has only to know the branching ratios into $K\bar{K}$, $\eta\eta$, $\rho\rho$, $\omega\omega$ and even K^*K^* above the corresponding thresholds, which can be deduced from Ref. [7]. For the decays into ρ's, ω's and K^*'s, we have taken into account the finite width of these particles. The various branching ratios in the range from 200 MeV to 2.5 GeV are shown in Fig.1.

Many channels are open when $M_H > 2$ GeV and the final states should not differ drastically from the "perturbative" ones (gg, $q\bar{q}g$ + fragmentation). To choose the transition mass value, we ask the branching ratios into strangeness and the final-state charged multiplicities to be identical in both non-perturbative and perturbative treatments. This transition occurs at $M_H \sim 2$ GeV.

Near the decay thresholds of $2m_D$ and $2m_B$, the partial widths are largely enhanced by virtual vertex corrections. Moreover, if the Higgs boson is heavy enough, a quark coming from its decay may radiate a gluon energetic enough to produce a third jet, thereby modifying the event topology. Thus, first order QCD corrections have been determined [6, 8] and included in our simulation.

4. SIMULATION OF $Z^\circ \to H^\circ Z^*$ ($Z^* \to e+e-, \mu+\mu-, \tau+\tau-, \nu\bar{\nu}, q\bar{q}(g)$)

The cross section for H° production from $Z^\circ \to H^\circ Z^*$ where $Z^* \to e^+e^-$, $\mu^+\mu^-$, $\tau^+\tau^-$, $\nu\bar{\nu}$ and $q\bar{q}(g)$ is based on the calculation in Ref. [9] for the production of H° $\mu^+\mu^-$ at the Z°. The Born approximation without initial-state radiation from Ref. [9] is then replaced by the equivalent "improved Born approximation" [10] and convoluted with an initial-state radiation spectrum calculated to second order [11].

The simulated events for $Z^\circ \to H^\circ Z^*$ are processed by the same reconstruction and analysis programs as used for the real data. The simulation includes initial-state radiation of a photon. For the channels $H^\circ e^+e^-$, $H^\circ \mu^+\mu^-$, $H^\circ \tau^+\tau^-$ final-state radiation of a photon from the leptons is also included using an algorithm given by Ref. [12]; and in the case of $Z^\circ \to H^\circ q\bar{q}(g)$, the LUND parton-shower model (version 6.3) [13] is used for the $q\bar{q}(g)$ fragmentation. For the Higgs decay we use the simulation program as described in section 3. Trigger efficiencies are calculated using a Monte Carlo simulation program which models the trigger conditions of the ALEPH detector and has been tuned to and tested with the data from the processes $Z^\circ \to e^+e^-$, $\mu^+\mu^-$, $\tau^+\tau^-$ and hadrons.

5. SEARCH FOR THE SHORT-LIVED HIGGS BOSON

We present here the method of a comprehensive search for a Higgs boson between 212 MeV (two muon threshold) and about 15 GeV by using the processes $Z^\circ \to H^\circ Z^*$. Sections 5.1 to 5.3 give the descriptions of how to identify events of the type $Z^\circ \to H^\circ Z^*$ and the decay products of the Higgs candidates, and most important of all, how to reject background events from photon-photon interactions, beam gas interactions and Z° decays. At least $3 pb^{-1}$ of simulated data have been produced for the background processes $Z^\circ \to e^+e^-$, $\mu^+\mu^-$, $\tau^+\tau^-$ and $q\bar{q}(g)$, as well as the two-photon interactions ($\gamma\gamma \to e^+e^-$, $\mu^+\mu^-$, $\tau^+\tau^-$ and hadrons), using the full detector simulation. They are used as an important guide to devise the event selection criteria as listed below.

Unless otherwise specified, throughout this section a charged particle is required to have 4 TPC coordinates and $|d_0|$ smaller than 4 cm and $|z_0|$ smaller than 7 cm, where d_0 is defined as the distance of closest approach to the interaction point on the plane perpendicular to the beam axis and z_0 is the distance from the interaction point along the beam axis.

5.1 *SELECTION OF EVENTS FOR $Z^\circ \rightarrow H^\circ \nu\bar{\nu}$*

The decay channel $Z^\circ \rightarrow H^\circ \nu\bar{\nu}$ provides the best means to search for a Higgs over a wide range of Higgs masses. For a light Higgs, the signal is a monojet with large missing energy and momentum. The event selection criteria are given here:

(1) The event is required to have a minimum of two oppositely-charged particles and the total charge of the event should not exceed ± 4.

(2) The angle between the beam axis and the sphericity axis of the event, calculated with charged particles only, must be greater than 40°.

(3) The magnitude of the vector sum of the transverse momenta of all charged particles with respect to the beam axis must be greater than 2 GeV/c.

(4) $\cos\theta_{max} > -0.1$.
θ_{max} is the maximum angle between any charged particle with momentum greater than 0.3 GeV/c and the direction of the vector sum of the momenta of all charged particles.

(5) $\cos\theta_{jet\text{-}jet} > -0.1$.
The event is divided into two hemispheres, by using the plane perpendicular to its sphericity axis, in the rest system of all charged particles. Charged particles in each hemisphere then define a jet. In the laboratory system, the vector sum of the momenta of all the charged particles in each jet gives the jet axis and $\theta_{jet\text{-}jet}$ is the angle between these two jet axes.

(6) The events which satisfy the selection criteria (1) to (5) are monojet-like. Consider all the ECAL modules in the hemisphere opposite to the direction of the monojet (defined by the vector sum of the momenta of the charged particles). The event is rejected if the energy deposition of any module exceeds 2 GeV. Similarly, events are rejected if the total energy in LCAL exceeds 5 GeV. From a study of the randomly triggered events, this requirement on the LCAL energy introduces a 1.5% inefficiency to the acceptance of the Higgs events.

Selection criteria (2) and (3) remove background from two-photon and beam gas interactions, while (4), (5) and (6) primarily remove the background from $Z^\circ \rightarrow q\bar{q}(g)$. Selection criterion (4) defines the monojet and is the most powerful cut. Fig. 2(a) shows the $\cos\theta_{max}$ distribution for the data and Fig. 2(b) for the Monte Carlo simulation for Higgs mass of 5 GeV after the selection criteria (1), (2), (3) and (6) have been applied. The cut is at $\cos\theta_{max} = -0.1$. Applying the additional selection criterion (5) to the data, no event survives.

5.2 SELECTION OF EVENTS FOR $Z^\circ \rightarrow H^\circ e^+e^-$, $Z^\circ \rightarrow H^\circ \mu^+\mu^-$, $Z^\circ \rightarrow H^\circ \tau^+\tau^-$

The topologies of the decay modes $Z^\circ \rightarrow H^\circ e^+e^-$, $Z^\circ \rightarrow H^\circ \mu^+\mu^-$ and $Z^\circ \rightarrow H^\circ \tau^+\tau^-$ are simple. However, the rates of these decay modes are low and in particular the contribution from $Z^\circ \rightarrow H^\circ \tau^+\tau^-$ is minimally useful due to the softer momentum spectrum in tau decay. The selection criteria are:

(1) Two oppositely charged particles are required to form a Z^* candidate, each with at least 15 GeV/c momentum; the cosine of the angle between them is required to be smaller than 0.1. If more than one pair of charged particles satisfies this requirement, the pair with the highest energy is chosen.

(2) The remaining charged particles are assigned to the Higgs candidate. Their number must be at least 2, each with $|d_0| < 3$cm and $|z_0| < 10$cm.

(3) To reject backgrounds of the types $Z^\circ \rightarrow q\bar{q}(g)$ and $Z^\circ \rightarrow \tau^+\tau^-$, the cosine of the angle between the most energetic charged particle of the Higgs candidate and either of the charged particles of the Z* candidate is required to be less than 0.9.

(4) If the Higgs candidate has only two charged particles, they must be of opposite charge and at least one of the particles must have a momentum greater than 1 GeV/c. A pair-finder algorithm is applied to reject events with the two particles consistent with an e^+e^- pair from a converted photon. The efficiency of this algorithm for finding converted pairs where both 'secondary' charged particles are reconstructed in the TPC is 84%. It introduces only a 9% inefficiency for a Higgs mass of 300 MeV, for example.

With the above event selection criteria, three events survive. The invariant masses of the charged particles in the Higgs candidates of those events exceed 25 GeV (two events are expected from the background process $Z^\circ \rightarrow q\bar{q}(g)$). Hence, no event survives in the mass range of this search (below 15 GeV).

5.3 *SELECTION OF EVENTS FOR $Z^\circ \rightarrow H^\circ q\bar{q}(g)$*

For a Higgs with mass above a few GeV, the events where the Z* decays into $q\bar{q}$ are difficult to use because of the QCD background involving three or four jets. However, a Higgs of 2 GeV mass or less has a sizeable branching ratio into two particles and can be efficiently identified. In this analysis, we restrict our search to a Higgs boson decaying into two charged particles. The event selection criteria are:

(1) All particles, both charged and neutral, are projected onto the event plane. The event plane is the plane formed by the two eigenvectors, corresponding to the two larger eigenvalues, of the sphericity tensor. The use of event plane is motivated by the fact that the three particles from the Z° decay lie on a plane. A neutral particle is defined as an electromagnetic cluster in the ECAL which is not associated with a charged particle. The energy of each

charged or neutral particle must be greater than 300 MeV. The LUND cluster algorithm [14] is applied to the momenta projected on this event plane. Only events with the number of jets equal to 3 or 4 are accepted.

(2) The jet with the smallest multiplicity is assigned to be the candidate for the "Higgs jet". The event is kept only if the multiplicity of the "Higgs jet" is 2 or 3. For each charged particle i in the "Higgs jet", let $P_{\perp i}$ be the minimum transverse momentum with respect to all other jets. The two oppositely charged particles from the "Higgs jet" with the largest $P_{\perp i}$ are selected to be the two-prong decay products of the Higgs candidate. Each $P_{\perp i}$ must be greater than 800 MeV/c and the sum of the energies of the two particles must be greater than 3 GeV.

(3) The angle between two highest multiplicity jets is required to be greater than 125°.

(4) A cone with half angle $\theta = 45.6°$ is formed with respect to the momentum of the $H°$ candidate (the vector sum of the momenta in the three-dimensional space of the two charged particles designated as the Higgs decay products). Events are kept only if the sum of the longitudinal momentum components along the direction of the $H°$ candidate is less than 500 MeV/c for all other charged particles in the cone.

(5) For the study of the low mass Higgs boson, a powerful variable is the ratio of $P_{\perp H°}$ to $M_{H°}$ where $P_{\perp H°}$ is the minimum transverse momentum of the Higgs candidate with respect to all other jets on the event plane and $M_{H°}$ is the invariant mass of the Higgs candidate. In this calculation, the electron mass is assumed for each of the two charged particles. Events are rejected inside a box defined by the ratio $P_{\perp H°} / M_{H°}$ less than 12 and $P_{\perp H°}$ less than 9 GeV/c.

Applying the selection criteria (1) to (5) to the data, no event survives.

5.4 ESTIMATION OF THE NUMBER OF EVENTS EXPECTED FROM $Z^\circ \to H^\circ Z^*$ AND SYSTEMATIC ERRORS

Events at twelve different Higgs masses have been simulated for this analysis according to the description given in section 4. Table 1 gives the detection efficiency and the expected event numbers at different Higgs masses. The corrections due to different production cross-sections at different total center-of-mass energies are taken into account. The systematic errors on the expected number of $Z^\circ \to H^\circ Z^*$ events are estimated to be: less than 3% from the integrated luminosity, 10% corresponding to uncertainties in the cross section calculation and 1% to 5% for trigger efficiencies at different Higgs masses. In addition, by varying the values of variables used in the event selection criteria over a reasonable range, we find that the uncertainty in the efficiency due to the event selection criteria varies from 2% to less than 10%. Combining all errors in quadrature, we find that the maximum systematic error for the expected number of events for the combined processes $Z^\circ \to H^\circ Z^*$ ($Z^* \to e^+e^-, \mu^+\mu^-, \tau^+\tau^-, \nu\bar{\nu}, q\bar{q}(g)$) is $\pm$ 15%. For the mass range between the two-pion threshold to about 3 GeV, an additional uncertainty of $\pm$15% comes from the decay branching ratio.

5.5 RESULTS ON THE SEARCH FOR THE SHORT-LIVED HIGGS BOSON

After applying the selection criteria given in sections 5.1 to 5.3, we find that no event survives in our data sample. Fig.3 shows the number of events expected from the sum, as well as the individual processes, for $Z^\circ \to H^\circ e^+e^-$, $Z^\circ \to H^\circ \mu^+\mu^-$, $Z^\circ \to H^\circ \tau^+\tau^-$, $Z^\circ \to H^\circ \nu\bar{\nu}$ and $Z^\circ \to H^\circ q\bar{q}(g)$ as a function of the Higgs masses. To set mass limit in a conservative way, we reduce the number of expected events by 15% (21% for mass between $2M_\pi$ to 3 GeV) to take into account the systematic error. The mass range from 212 MeV to 15 GeV for the neutral Higgs boson is excluded at 95% C.L.

6. SEARCH FOR THE LONG-LIVED LIGHT HIGGS BOSON

Since the Higgs boson of the Standard Model with a mass less than 212 MeV is long-lived and decays predominantly into an e^+e^- pair, special analysis methods are devised to make use of these characteristics. Two methods are used for this search.

6.1 METHOD 1: EXTENSION OF THE METHOD USED FOR THE SHORT-LIVED HIGGS BOSONS

The analysis method described in section 5 can easily be extended into the mass region below 212 MeV. For the $Z^\circ \to H^\circ \nu\bar{\nu}$ channel, in addition to the application of the event selection criteria (1) to (6) of section 5.1, we require that there are only two oppositely charged particles in an event. To allow the more efficient detection of particles coming from a displaced vertex, we remove the requirements of d_0 and z_0 for one of the two charged particles and require that $|d_0| < 7$ cm and $|z_0| < 10$ cm for the other. No event survives in the search for this channel. For the $Z^\circ \to H^\circ q\bar{q}(g)$ channel, no additional requirement is needed to extend the analysis method as described in section 5.3. Again no event is found for the search below 212 MeV. Due to the radiative Bhabha and μ-pair backgrounds, the search for the channels $Z^\circ \to H^\circ e^+e^-$, $Z^\circ \to H^\circ \mu^+\mu^-$ and $Z^\circ \to H^\circ \tau^+\tau^-$ is not used for this mass region. Table 2 gives the detection efficiency and the expected event numbers for 5 different Higgs masses below 212 MeV. From the sum of the two channels, and taking into account a $\pm 15\%$ systematic errror, we exclude the existence of a Higgs boson in the mass range from 50 MeV to 212 MeV at 95% C.L.

6.2 METHOD 2: THE METHOD OF ISOLATED VERTICES

In this method, we make use of the characteristic decay point displaced from the e^+e^- interaction point. Typically, when produced in Z° decays, a 100 MeV Higgs would travel over a distance of 100 cm and would therefore be detected and measured in the TPC. Consequently, this search method relies exclusively on the observation of a decay into two oppositely-charged particles (V°) away from the interaction point, independently of the accompanying final state whether it be $\ell^+\ell^-$ (ϵ, μ, τ), $\nu\bar{\nu}$, or hadrons.

Events are selected if a V° can be reconstructed from two TPC tracks with momenta larger than 0.2 GeV/c and a total momentum larger than 2 GeV/c. The decay point is required to be at least 20 cm away from the interaction point in the plane transverse to the beams, with the V° momentum vector pointing back to the origin to better than 5°. Events are then classified according to the number of extra charged particles (N_{tr}) originating from the interaction point. We require each V° to be isolated in space; no other charged particle is allowed if it is emitted in a 20° cone around the V° momentum vector. Finally, to avoid background from beam-gas or photon-photon interactions, the scalar sum of the momenta of the extra charged particles is required to exceed 10 GeV/c for events with N_{tr} larger than one.

The selection procedure yields 187 events for all topologies. The rest of the analysis proceeds differently for the three channels as the backgrounds are of a different nature.

(1) For the 25 $H^\circ\nu\bar{\nu}$ candidates, we require an energy deposition less than 5 GeV in LCAL or a transverse momentum of the V° with respect to the beam larger than 2 GeV/c, to remove small-angle Bhabha events with a radiated photon converted in the detector. Events with a large (> 30 GeV) electromagnetic shower opposite to the V° are also removed.

(2) For the $H^\circ\ell^+\ell^-$ candidates, as well as for the hadronic events to be discussed next, one has to consider a background from pair-converted photons. Since these photons are more likely to convert into an e^+e^- pair in the region between the ITC and the TPC with a thickness of 3.3% radiation lengths, for these channels the decay region is further limited to the TPC gas volume, at least 40 cm away from the interaction point in the transverse plane. Of the nine leptonic candidates, only one survives.

(3) As expected, the selected sample of 130 $H^\circ q\bar{q}(g)$ candidates contains a large component from decays of K_S, Λ and $\bar{\Lambda}$, which are

rejected if the $\pi^+\pi^-$ mass, or the $p\pi^-$ or the $\bar{p}\pi^+$ masses, lie in the ranges 470-530 MeV or 1110-1120 MeV, respectively. Events are further removed if both V° tracks are identified as hadrons in the calorimeter or if the V° momentum is smaller than 3.5 GeV/c.

Only one event of the type $Z^\circ \to e^+e^-V^\circ$, $V^\circ \to e^+e^-$ remains as a light Higgs candidate. The measured mass of this event is 102±40 MeV and the transverse momentum of the pair with respect to the beam direction is 5.1 GeV/c. With our data selection we expect 0.4 events of the type $\ell^+\ell^-\gamma$ where the photon converts into a pair in the TPC gas volume.

The Higgs detection efficiency is largely determined by the requirement of observing the actual decay inside the useful volume of the TPC. This causes the efficiency to decrease on each end of the studied mass range. The V° reconstruction efficiency within the decay region is studied with a full simulation of the detector and is determined to be 0.78±0.04 for the $H^\circ\nu\bar{\nu}$ channel and 0.72±0.04 for the others.

To determine the efficiency relative to the V° isolation cut for hadronic events, we used a method based on data rather than on Monte Carlo simulation. The actual $Z^\circ \to$ hadrons events from our data are Lorentz-boosted opposite to a fake Higgs particle randomly generated in space. The energies of the overall "event" are then appropriately rescaled to restore the correct centre-of-mass energy. The final Higgs energy is chosen to follow the expected distribution from the Z° decay. The corresponding efficiency varies from 0.71 to 0.76 for Higgs masses between 30 and 212 MeV. Finally, a correction is applied to take into account the K° and Λ° mass cuts.

The overall efficiencies and expected event numbers for the different channels are given in Table 3. Summing up all channels as shown in this table, taking into account the one candidate event and a systematic error of ±15% (same as given in section 5.4), we exclude the existence of the Higgs boson in the mass range from 32 MeV to 212 MeV at 95% C.L.

6.3 COMBINED RESULT FOR THE LONG-LIVED LIGHT HIGGS BOSON

While method 1 is more efficient for Higgs mass above 100 MeV, method 2 is more sensitive for the lower masses. Fig.4 shows the expected number of events for both methods and the solid curve gives the best value of the two. The 95% C.L. limit is indicated.

7. CONCLUSION

A search for the neutral Higgs boson is performed based on the processes $Z^\circ \rightarrow H^\circ e^+e^-$, $H^\circ \mu^+\mu^-$, $H^\circ \tau^+\tau^-$, $H^\circ \nu\bar{\nu}$ and $H^\circ q\bar{q}(g)$ using 542 nb^{-1} of data collected by the ALEPH detector. Fig.5 gives the number of events expected from the sum, as well as the individual processes, as a function of the Higgs boson mass over the full region of search. While the process $Z^\circ \rightarrow H^\circ \nu\bar{\nu}$ provides the most powerful means for this search, the result of combining all the processes excludes the neutral Higgs boson over the mass range from 32 MeV to 15 GeV at 95% C.L. and 40 MeV to 12 GeV at 99% C.L. This result is obtained within the context of the Standard Model with no further assumption.

8. ACKNOWLEDGEMENTS

We thank the LEP Division for the extraordinary start-up performance of the LEP machine. Those of us from the non-member countries thank CERN for its hospitality.

9. REFERENCES

[1] S.L. Glashow, Nucl. Phys. **22** (1961) 579;
S. Weinberg, Phys. Rev. Lett. **19** (1967) 1264;
A. Salam, Proc. Eighth Nobel Symp., ed. N. Svartholm (Almqvist and Wiksell, Stockholm, 1968) p.367.

[2] P.W. Higgs, Phys. Lett. **12** (1964) 132;
Phys. Rev. Lett. **13** (1964) 508;
Phys. Rev. **145** (1966) 1156;
F. Englert and R. Brout, Phys. Rev. Lett. **13** (1964) 321;
G.S. Guralnik, C.R. Hagen and T.W.B. Kibble, Phys. Rev. Lett. **13** (1964) 585;
T.W.B. Kibble, Phys. Rev. **155** (1967) 1554.

[3] S.J. Freedman *et al.*, Phys. Rev. Lett. **52** (1984) 240;
I. Beltrami *et al.*, Nucl. Phys. **A451** (1986) 679;
N. Baker *et al.*, Phys. Rev. Lett. **59** (1987) 2832;
P. Franzini *et al.*, CUSB Collaboration, Phys. Rev. **D35** (1987) 2883;
S. Egli *et al.*, Phys. Lett. **222B** (1989) 533;
P. Yepes, Phys. Lett. **227B** (1989) 182;
M. Davier and H. Nguyen Ngoc, Phys. Lett. **229B** (1989) 150;
P. Yepes, Phys. Lett. **229B** (1989) 156;
A. Snyder *et al.*, Phys. Lett. **229B** (1989) 169;
M.S. Alam *et al.*, CLEO Collaboration, Phys. Rev. **D40** (1989) 712;
R.N. Cahn, Rep. Prog. Phys. **52** (1989) 389;
M.S. Atiya *et al.*, preprint BNL-43212, PRINCETON/HEP 89-01, TRI-PP-89-70;
G.D. Barr *et al.*, (1989), CERN-EP/89-156, to be published in Phys. Lett. B.

[4] ALEPH Collaboration, ALEPH: A detector for electron-positron annihilations at LEP, to be published in Nucl. Inst. Meth.

[5] P. Janot, LAL 88-65 (1988).

[6] P.J. Franzini *et al.*, in *Z Physics at LEP 1*, CERN 89-08, Vol. 2, p.59 eds. G. Altarelli, R. Kleiss and C. Verzegnassi.

[7] M. Voloshin and V. Zakharov, Phys. Rev. Lett. **45** (1980) 688;
M. Voloshin, Sov .J. Phys. **44** (3) (1986) 478;
S. Raby and G.B. West, Phys. Rev. **D38** (1988) 3488.

[8] P. Janot, Phys. Lett. **223B** (1989) 110.

[9] F.A. Berends and R. Kleiss, Nucl. Phys. **B260** (1985) 32.

[10] M. Consoli *et al.*, in *Z Physics at LEP1*, CERN 89-08 Vol. 1, p.7, eds. G. Altarelli, R. Kleiss and C. Verzegnassi;
D.C. Kennedy and B.W. Lynn, Nucl. Phys. **B322** (1989) 1;
W. Hollik and R. Kleiss, private communication.

[11] O. Nicrosini and L. Trentadue, Phys. Lett. **196B** (1987) 551.

[12] R. Kleiss, Phys. Lett. **180B** (1986) 400.

[13] M. Bengtsson, T. Sjöstrand, Phy. Lett. **185B** (1987) 435;
T. Sjöstrand and M. Bengtsson, Comp. Phys. Comm. **43** (1987) 367;
M. Bengtsson and T. Sjöstrand, Nucl. Phys. **B289**, 810 (1987).

[14] T. Sjöstrand, Comp. Phys. Comm. **28**, (1983) 229. In the algorithm, the jet-forming cutoff parameter d_{join} is changed from its default value to d_{join} = 2.0 GeV.

TABLE 1

Detection Efficiency (Eff.) and Number of Expected Events (N) as a Function of Higgs Mass

M_{H° (MeV)	$H^\circ e^+e^-$ $H^\circ\mu^+\mu^-$ $H^\circ\tau^+\tau^-$		$H^\circ\nu\bar{\nu}$		$H^\circ q\bar{q}(g)$		Total
	Eff.	N	Eff.	N	Eff.	N	ΣN
212	0.279	4.7	0.404	13.5	0.166	19.3	37.5
260	0.271	4.5	0.426	14.2	0.177	20.5	39.2
500	0.240	3.9	0.296	9.5	0.099	11.1	24.5
800	0.218	3.3	0.262	8.0	0.061	6.4	17.7
1200	0.216	3.0	0.237	6.6	0.059	5.7	15.3
2000	0.323	3.7	0.346	8.0	0.021	1.6	13.3
3000	0.403	3.8	0.478	9.1			12.9
4000	0.411	3.3	0.522	8.3			11.6
5000	0.418	2.9	0.534	7.3			10.2
10000	0.447	1.7	0.570	4.2			5.9
12000	0.456	1.4	0.561	3.4			4.8
15000	0.465	1.1	0.545	2.5			3.6

TABLE 2

Detection Efficiency (Eff.) and Number of Expected Events (N) as a Function of Higgs Mass

M_{H° (MeV)	$H^\circ \nu\bar{\nu}$		$H^\circ q\bar{q}(g)$		Total
	Eff.	N	Eff.	N	ΣN
50	0.057	1.9	0.015	1.8	3.7
60	0.081	2.8	0.018	2.1	4.9
80	0.127	4.3	0.033	3.9	8.2
100	0.202	6.8	0.044	5.2	12.0
200	0.350	11.8	0.104	12.1	23.9

TABLE 3

Detection Efficiency (Eff.) and Number of Expected Events (N) as a Function of Higgs Mass

M_{H° (MeV)	$H^\circ e^+e^-$ $H^\circ \mu^+\mu^-$ $H^\circ \tau^+\tau^-$		$H^\circ \nu\bar{\nu}$		$H^\circ q\bar{q}(g)$		Total
	Eff.	N	Eff.	N	Eff.	N	ΣN
25	0.036	0.6	0.021	0.7	0.016	1.9	3.2
50	0.102	1.7	0.073	2.5	0.051	6.0	10.2
100	0.137	2.3	0.169	5.7	0.093	10.9	18.9
150	0.103	1.7	0.190	6.4	0.077	9.0	17.1
200	0.068	1.2	0.160	5.4	0.051	5.9	12.5

FIGURE CAPTIONS

Fig.1 Branching ratios of the Higgs decays in the nonperturbative QCD mass range.

Fig.2 $\cos\theta_{max}$ distribution for (a) data and (b) Monte Carlo simulation of $Z^\circ \to H^\circ \nu\bar{\nu}$ for 5 GeV Higgs mass, both after applying the selection criteria (1), (2), (3) and (6) of section 5.1. (See section 5.1 for definition of $\cos\theta_{max}$). The cut is at $\cos\theta_{max} = -0.1$. The distribution in (b) is normalized to the data.

Fig.3 The number of events expected above 212 MeV for $Z^\circ \to H^\circ \ell^+ \ell^-$, ($e^+e^-$, $\mu^+\mu^-$ and $\tau^+\tau^-$), $Z^\circ \to H^\circ \nu\bar{\nu}$, $Z^\circ \to H^\circ q\bar{q}(g)$ and the sum of all the above channels as a function of the Higgs mass. The 95% C.L. limit is indicated corresponding to zero observed candidates.

Fig.4 The total number of events expected below 212 MeV for $Z^\circ \to H^\circ Z^*$ ($Z^* \to e^+e^-$, $\mu^+\mu^-$, $\tau^+\tau^-$, $\nu\bar{\nu}$ and $q\bar{q}(g)$) for Method 1 and Method 2 as a function of the Higgs mass. The solid curve follows the best value of the two. The 95% C.L. limit is indicated corresponding to one observed event below 100 MeV and zero above.

Fig.5 The number of events expected for $Z^\circ \to H^\circ \ell^+ \ell^-$, ($e^+e^-$, $\mu^+\mu^-$ and $\tau^+\tau^-$), $Z^\circ \to H^\circ \nu\bar{\nu}$, $Z^\circ \to H^\circ q\bar{q}(g)$ and the sum of all the above channels as a function of the Higgs mass. The 95% C.L. limit is also indicated corresponding to one observed candidate below 100 MeV and zero above 100 MeV, giving the excluded region of 32 MeV to 15 GeV.

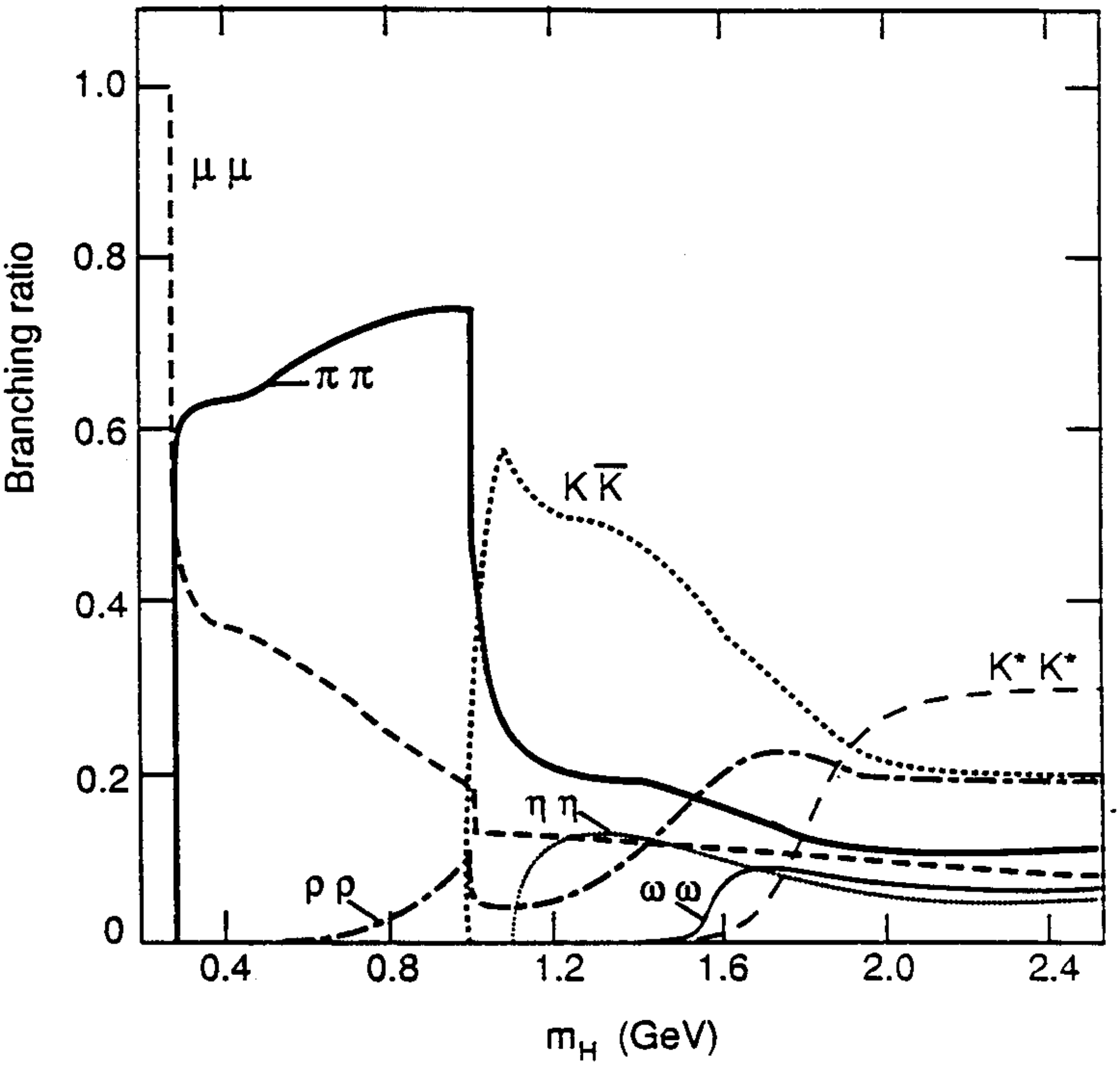

Branching ratio
1.0
0.8
0.6
0.4
0.2
0
μ μ
π π
K K̄
K* K*
η η
ρ ρ
ω ω
0.4
0.8
1.2
1.6
2.0
2.4
m_H (GeV)

Fig. 1

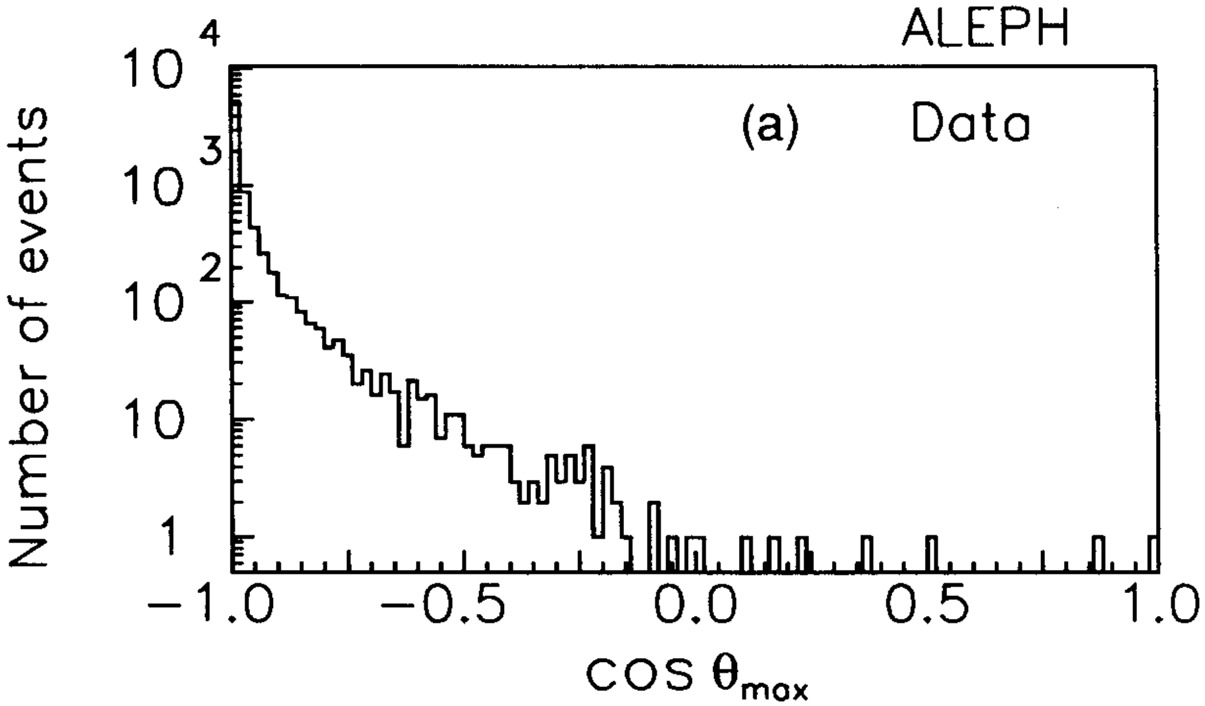
ALEPH
(a) Data
Number of events
10^4
10^3
10^2
10
1
−1.0
−0.5
0.0
0.5
1.0
cos θmax

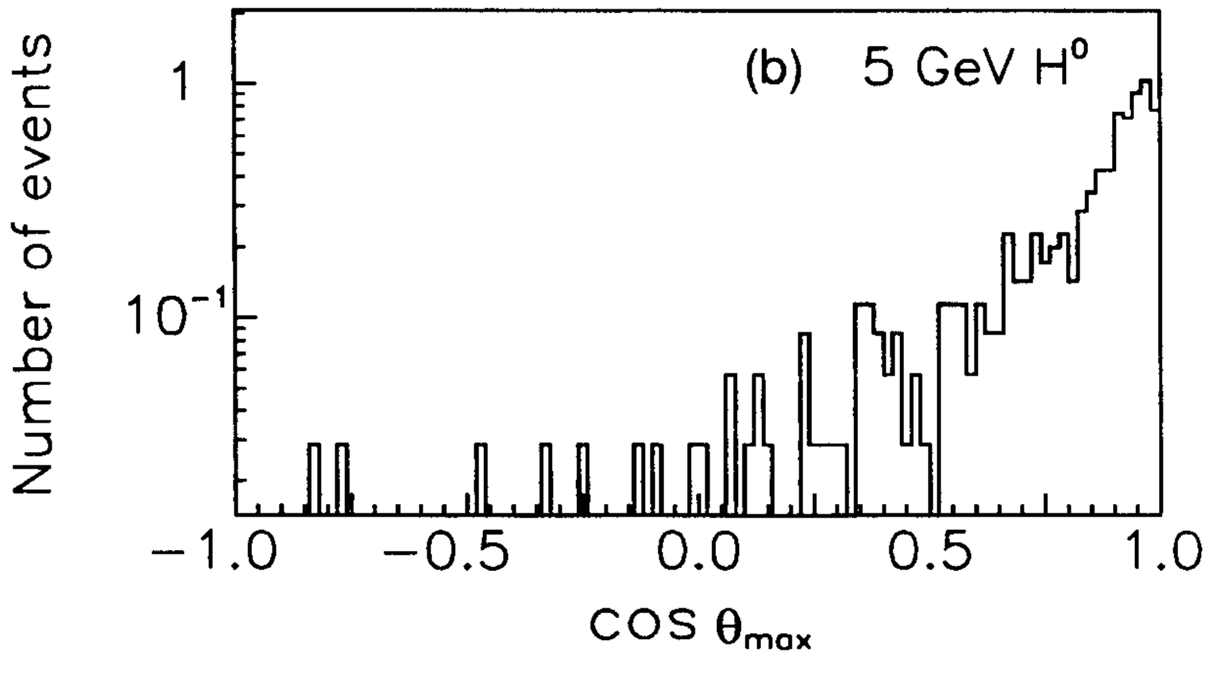
(b) 5 GeV H⁰
Number of events
1
10⁻¹
−1.0
−0.5
0.0
0.5
1.0
cos θmax

Fig. 2

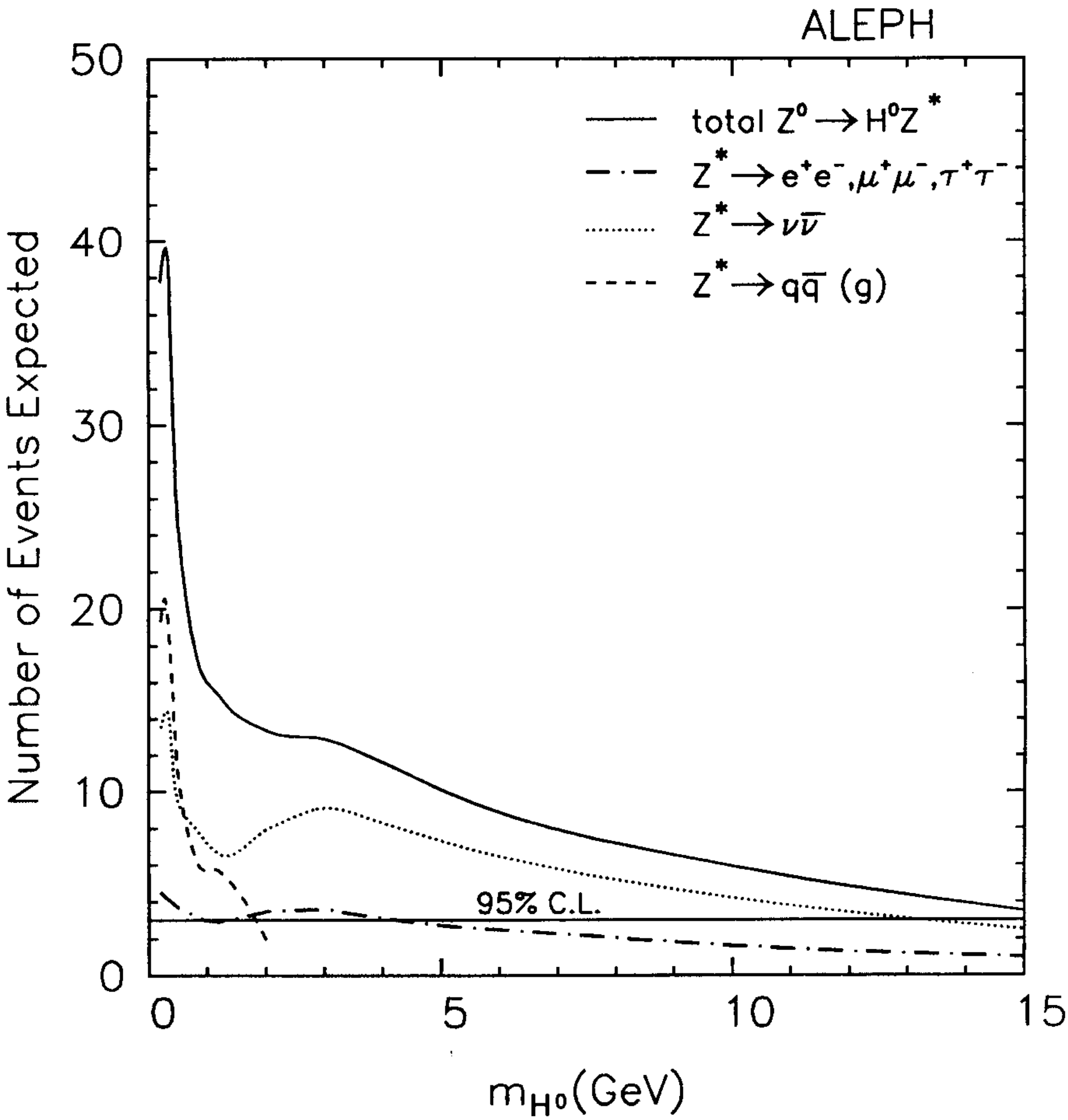
ALEPH
total $Z^0 \to H^0 Z^*$
$Z^* \to e^+e^-, \mu^+\mu^-, \tau^+\tau^-$
$Z^* \to \nu\bar{\nu}$
$Z^* \to q\bar{q}$ (g)
95% C.L.
Number of Events Expected
m_{H^0}(GeV)
0
10
20
30
40
50
0
5
10
15

Fig. 3

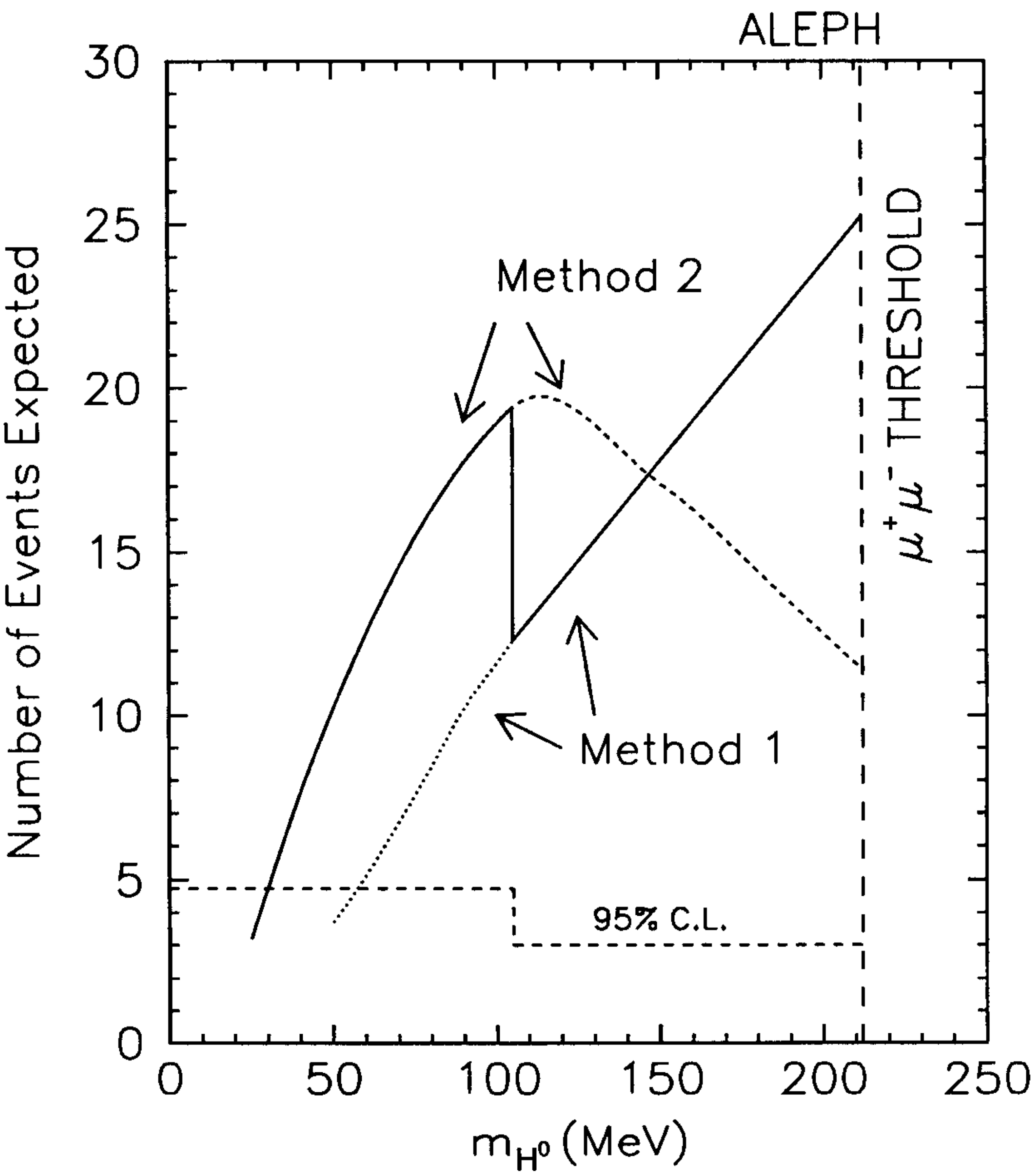
ALEPH
30
25
20
15
10
5
0
Number of Events Expected
Method 2
Method 1
95% C.L.
μ⁺μ⁻ THRESHOLD
0
50
100
150
200
250
m_H⁰ (MeV)

Fig. 4

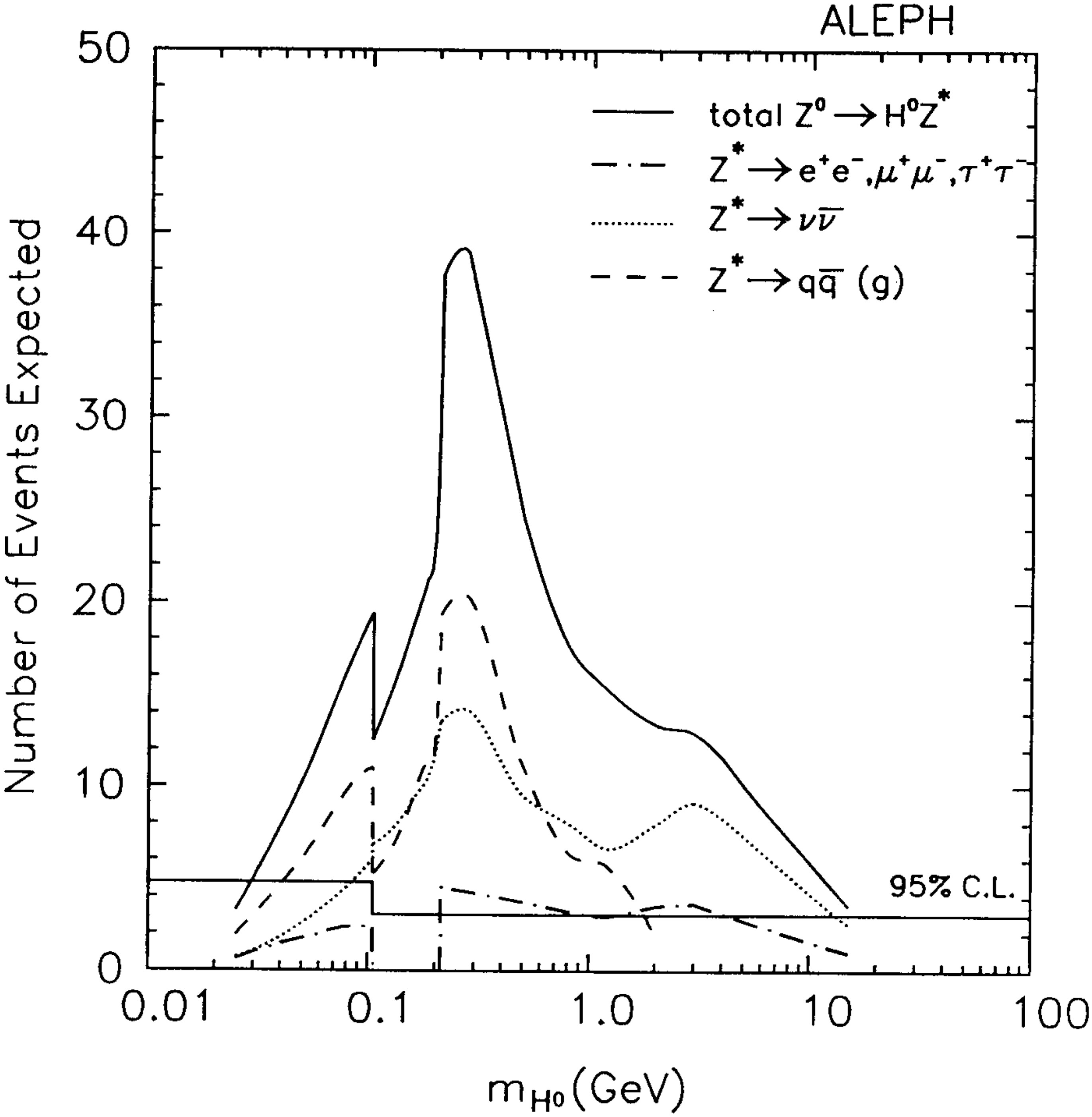

ALEPH
Number of Events Expected
50
40
30
20
10
0
0.01
0.1
1.0
10
100
m_{H^0}(GeV)
total $Z^0 \to H^0 Z^*$
$Z^* \to e^+e^-, \mu^+\mu^-, \tau^+\tau^-$
$Z^* \to \nu\bar{\nu}$
$Z^* \to q\bar{q}$ (g)
95% C.L.

Fig. 5